scientific reports

Check for updates

OPEN

Physiological resilience of intertidal chitons in a persistent upwelling coastal region

Carolina Fernández[1], María Josefina Poupin[1,2,3], Nelson A. Lagos[4,5], Bernardo R. Broitman[5,6] & Marco Antonio Lardies[5,6]✉

Current climate projections for mid-latitude regions globally indicate an intensification of wind-driven coastal upwelling due to warming conditions. The dynamics of mid-latitude coastal upwelling are marked by environmental variability across temporal scales, which affect key physiological processes in marine calcifying organisms and can impact their large-scale distribution patterns. In this context, marine invertebrates often exhibit phenotypic plasticity, enabling them to adapt to environmental change. In this study, we examined the physiological performance (i.e., metabolism, Thermal Performance Curves, and biomass and calcification rates) of individuals of the intertidal mollusk *Chiton granosus*, a chiton found from northern Peru to Cape Horn (5° to 55°S). Our spatial study design indicated a pattern of contrasting conditions among locations. The Talcaruca site, characterized by persistent upwelling and serving as a biogeographic break, exhibited lower pH and carbonate saturation states, along with higher pCO_2, compared to the sites located to the north and south of this location (Huasco and Los Molles, respectively). In agreement with the spatial pattern in carbonate system parameters, long-term temperature records showed lower temperatures that changed faster over synoptic scales (1–15 days) at Talcaruca, in contrast to the more stable conditions at the sites outside the break. Physiological performance traits from individuals from the Talcaruca population exhibited higher values and more significant variability, along with significantly broader and greater warming tolerance than chitons from the Huasco and Los Molles populations. Moreover, marked changes in local abundance patterns over three years suggested population-level responses to the challenging environmental conditions at the biogeographic break. Thus, *C. granosus* from the Talcaruca upwelling zone represents a local population with wide tolerance ranges that may be capable of withstanding future upwelling intensification on the Southern Eastern Pacific coast and likely serving as a source of propagules for less adapted populations.

Keywords Metabolism, Thermal performance curve, Calcification, Ocean acidification, Abundance, Carbonate saturation, Upwelling, Warming

Ocean Warming (OW), Ocean Acidification (OA), and Deoxygenation (DO) are the main global change drivers affecting marine ecosystems[1–3]. However, the interplay and combined effects of such drivers on the physiology and adaptive responses of marine organisms at the population level remain poorly understood[4–7].

Coastal upwelling regions are productive ecosystems where cold, nutrient-rich subsurface waters rise to the surface along the shoreline. In addition to low temperature and O_2 levels, upwelled waters are characterized by low pH and calcium carbonate saturation states (Ω) as well as high partial pressure of CO_2 (pCO_2) and dissolved inorganic carbon (DIC) content[8–11].

Under current climate change scenarios, upwelling in eastern boundary ecosystems is expected to intensify[12–14]. Furthermore, coastal upwelling can be locally intensified by factors such as wind patterns and

[1]Laboratorio de Bioingeniería, Facultad de Ingeniería y Ciencias, Universidad Adolfo Ibáñez, Santiago, Chile. [2]Center of Applied Ecology and Sustainability (CAPES), Santiago, Chile. [3]Millennium Nucleus for the Development of Super Adaptable Plants (MN-SAP), Santiago, Chile. [4]Centro de Investigación E Innovación, Para El Cambio Climático (CiiCC), Facultad de Ciencias, Universidad Santo Tomás, Santiago, Chile. [5]Instituto Milenio de Socio-Ecología Costera (SECOS), Santiago, Chile. [6]Facultad de Artes Liberales, Universidad Adolfo Ibáñez, Santiago, Viña del Mar, Chile. [7]Carolina Fernández and María Josefina Poupin contributed equally. ✉email: marco.lardies@uai.cl

seafloor topography. Thus, present-day areas of intense upwelling serve as natural laboratories for studying global change drivers as forces of natural selection in the marine environment[11,15–17].

Among intertidal organisms, marine mollusks are some of the most sensitive to changes in pH, carbonate chemistry, and seawater temperature. Their physiological and life-history traits, together with their shell production, are negatively impacted by low pH, high pCO_2, and low Ω[3,18,19]. Although juveniles of mollusks may be vulnerable to shell dissolution following low Ω conditions, warming may mitigate the negative impact of acidified waters on calcification[20–22]. Surprisingly, some evidence shows that temperature and pCO_2 can act synergistically by elevating the rates of energy expenditure and affecting acclimation in bivalves[22]. Interactive effects between temperature and pCO_2 have also been demonstrated in oysters and mytilids[23–25] and in the early developmental stages of other invertebrates[19,26–28]. Experiments with various larval stages of the abalone *Haliotis rufescens* Swainson, 1822 did not find effects of high pCO_2 on gene expression related to shell formation. Instead, these experiments revealed a reduction of the thermal tolerance and survival ranges of some larval stages[29]. Additionally, Duarte et al. (2014) found an interaction between temperature and pCO_2 on shell dissolution in individuals of the mussel *Mytilus chilensis* Hupé, 1854[24]. Moreover, these factors can interact antagonistically and influence the oxygen uptake and aerobic scope of marine ectotherms[30]. However, the above-mentioned studies have rarely incorporated variability in the adaptation and acclimatization of organisms[30], or the geographic variation of different populations in their responses to these stressors[11,31,32].

The evaluation of organismal performance across different temperatures, known as thermal sensitivity, employs the Thermal Performance Curve (TPC). Different populations can exhibit variations in their thermal physiological performances depending on their geographical distribution and physiological state[33,34]. Standard Metabolic Rate (SMR), a temperature-dependent physiological variable in ectothermic animals, represents the minimum energy level required in an organism in the absence of activity, digestive processes, and physiological stress[16,32,35]. Evidence suggests that hypercapnia (i.e., the condition of elevated CO_2 levels in the environment) can impact metabolic processes[22,36]. Therefore, from an energy perspective, both thermal performance and metabolic rate serve as crucial parameters for assessing the impact of future environmental conditions of ocean acidification and warming on the physiology of organisms[37,38]. Finally, considering that low levels of Ω can affect shell production in calcifying organisms[28,39,40], the measurement of inorganic matter content is useful for estimating the body size and production of calcium carbonate[41].

Talcaruca, located on a large headland on the Chilean coast at 30°S (Punta Lengua de Vaca, PLV), experiences semi-permanent upwelling conditions. As a result, it serves as a biogeographic barrier for several marine species[31,38,42]. *Chiton granosus* (Freembly, 1827) is a primitive polyplacophore mollusk with a broad distribution, spanning the entire southeastern Pacific from 5 to 55°S and crossing this biogeographic break[43]. This intertidal chiton has eight valves mainly made of aragonite, is sedentary, and feeds by scraping the substrate with a radula reinforced with magnetite[44]. Living in the mid-high intertidal zone on rocky walls and platforms, this species is exposed to extreme temperature variations and hypoxia levels[36,45]. Additionally, chitons have an important ecological role as controllers of algal biomass[45], and they affect the succession community structure of the rocky intertidal zone[45].

Together with phenotypic plasticity[46,47], evolutionary adaptation is probably one of the main mechanisms by which populations can avoid extinction in a changing environment[48,49]. Nevertheless, little is known about plasticity patterns in calcifying organisms inhabiting the challenging conditions of upwelling zones, which are poised to intensify in the future. In this study, we hypothesized that chiton populations exposed to persistent upwelling conditions will show higher phenotypic plasticity and higher overall performance than populations from seasonal upwelling zones under experimental conditions simulating future environmental change.

Results

Oceanographic patterns

The three study sites are distributed over four degrees of latitude (Fig. 1a) and exhibit differences in ocean temperature patterns. All sites showed annual maxima during (Austral) mid-summer and minima by late winter – early spring (Fig. 1b). The more equatorward site (Huasco) was the warmest and showed a wider annual temperature range. In contrast, the coldest site was not the most poleward, but the central one (Talcaruca). The Talcaruca site showed the lowest annual minima, lowest annual maxima, and the smallest standard deviation for the coldest and warmest months (Table 1). Los Molles, the furthest poleward site, exhibited intermediate thermal patterns and had the largest standard deviations for both the warmest and coldest months (Table 2). Seasonal minima for all three sites were recorded during August, while maxima took place during February, except for Los Molles where it took place during January (Fig. 1b and Table 2). The autocorrelation pattern of temperature anomalies at each site indicated that the Talcaruca site had larger day-to-day variability over synoptic time scales (1–15 days, Fig. 1c) compared to the Huasco and Los Molles sites. Multivariate analysis of carbonate system parameters showed large contrasts between sites (Wilk's $\lambda = 0.085$; F-exact test = 9.708; $P < 0.001$). However, both Dunnet's C as post-hoc test for MANOVA and univariate ANOVAs of each environmental parameter did not show differences among sites. Talcaruca was characterized by low pH levels, being lower than those at the Huasco site and higher than those at the Los Molles site. Similarly, DIC, CO_3^{2-} and alkalinity levels were higher in Talcaruca (Table 2). Finally, while $\Omega_{calcite}$ was lower at Talcaruca, $\Omega_{aragonite}$ was similarly lower in Talcaruca and Los Molles. Only salinity followed a gradient, decreasing poleward (Table 2).

Biomass and shell carbonates content

Chitons from Los Molles and Huasco presented a Condition Index (CI) that remained almost constant with the length (L) of the individuals. For these localities, the slopes were not significantly different from zero for $\log_{10}$ transformed data (Los Molles: $CI = 0.04065L + 12.62$, $F_{1,27} = 0.4504$, $P = 0.5079$; Huasco: $CI = 0.009191L + 12.47$,

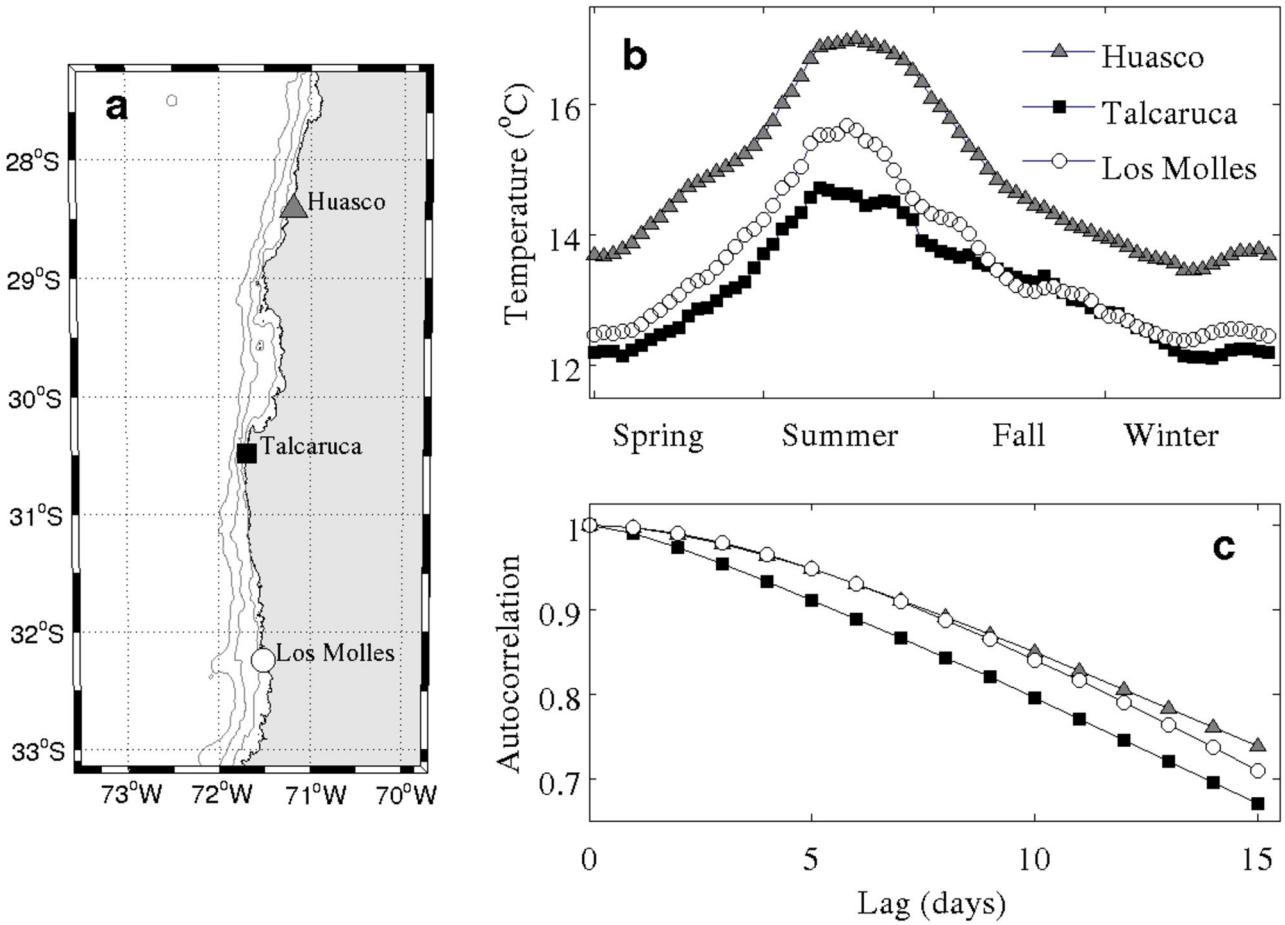

Fig. 1. (**a**) Map of the study locations along the north-central Chilean coastline. (**b**) Long-term mean daily sea surface temperatures (°C) at each study site, obtained from in situ measurements ranged from 8 to 17 years. (**c**) Autocorrelation of temperature anomalies at each site over synoptic time scales (1 – 45 days). Sites are represented as follows: grey triangle – Huasco, black square – Talcaruca, and white circle – Los Molles.

Site (lat long)	Latitude-Longitude	Minima (°C)	Maxima (°C)	Range (°C)
Huasco	– 28.41S-71.19W	13.56 ± 0.48	16.86 ± 0.6	3.30
Talcaruca	– 30.48S-71.7W	12.18 ± 0.34	14.54 ± 0.47	2.35
Los Molles	– 32.24S-71.52W	12.46 ± 0.61	15.36 ± 0.79	2.90

Table 1. Names, locations, and annual extremes of the climatologies shown in Fig. 1 ± 1 SD with maxima during Austral summer.

Carbonate System Parameter	Huasco	Talcaruca	Los Molles
Salinity (PSU)	34.15 ± 0.23	32.93 ± 1.08	32.44 ± 1.37
pH_{NBS}	8.09 ± 0.03	7.92 ± 0.31	8.02 ± 0.11
Total Alkalinity (mM kg^{-1} SW)	2293.91 ± 14.45	2323.12 ± 119.06	2261.27 ± 32.43
DIC (mM kg^{-1} SW)	2087.76 ± 61.16	2158.18 ± 146.46	1963.08 ± 95.89
CO_3^{2-} (mM kg^{-1} SW)	137.13 ± 57.03	147.78 ± 47.40	120.09 ± 27.40
pCO_2 (µatm)	466.74 ± 107.88	685.95 ± 602.47	567.73 ± 171.99
$\Omega_{calcite}$	3.03 ± 0.82	2.57 ± 1.13	2.90 ± 0.65
$\Omega_{aragonite}$	2.77 ± 0.64	1.89 ± 0.83	1.86 ± 0.42

Table 2. Salinity, pH and carbonate system parameters mean conditions (± SD) measured at the three study locations. The values correspond to 25 discrete samples collected during the field period (March 2015-December 2018).

$F_{1,29} = 0.06823$, $P = 0.7958$). Conversely, individuals from Talcaruca displayed a lower CI at larger lengths, with a negative slope significantly different from zero (CI = −0.5011*L + 54.05, $F_{27,50} = 27.50$) (Fig. 2a). The slopes from Huasco and Los Molles significantly differed from that of Talcaruca ($F_{2,86} = 19.05$, $P < 0.0001$) (Fig. 2a). In contrast, CI did not change with length for individuals from Huasco and Los Molles (Fig. 2a). The CI of individuals from Talcaruca was 87% and 104% higher than those from Los Molles and Huasco, respectively ($P < 0.001$) (Fig. 2b).

On average, the specimens from Talcaruca exhibited a size that was 51% greater than those from Los Molles ($P < 0.0001$) and 14% larger than those from Huasco ($P = 0.0272$) (Fig. 2c). Individuals from Huasco were also significantly larger (32% on average) than those from Los Molles ($P = 0.0011$) (Fig. 2c). Calcium carbonate content was proportional to length in all populations, with slopes significantly differing from zero ($P < 0.001$). The slope of the individuals from Los Molles was significantly different from the other two populations ($F_{2,86} = 14.08$, $P < 0.0001$), indicating that these individuals tended to have higher levels of shell carbonate than those from the other populations at similar lengths (Fig. 2c).

The Ash Free Dry Weight (AFDW), which represents the biologically active tissue weight in *C. granosus*, tended to increase in larger individuals across all populations, and all the slopes were significantly different from zero (Fig. 2d). The regression equations, for $\log_{10}$ transformed data, for AFDW were as follows: AFDW = 0.04488L-0.9550 for Huasco; AFDW = 0.04121L-0.8312 for Talcaruca and AFDW = 0.03501L-0.9828, for Los Molles. Additionally, the slopes among populations did not differ significantly, with a pooled slope equal to 0.03840 (Fig. 2d). Nevertheless, the intercepts were significantly different ($F_{2,88} = 49.41$, $P < 0.0001$). Data

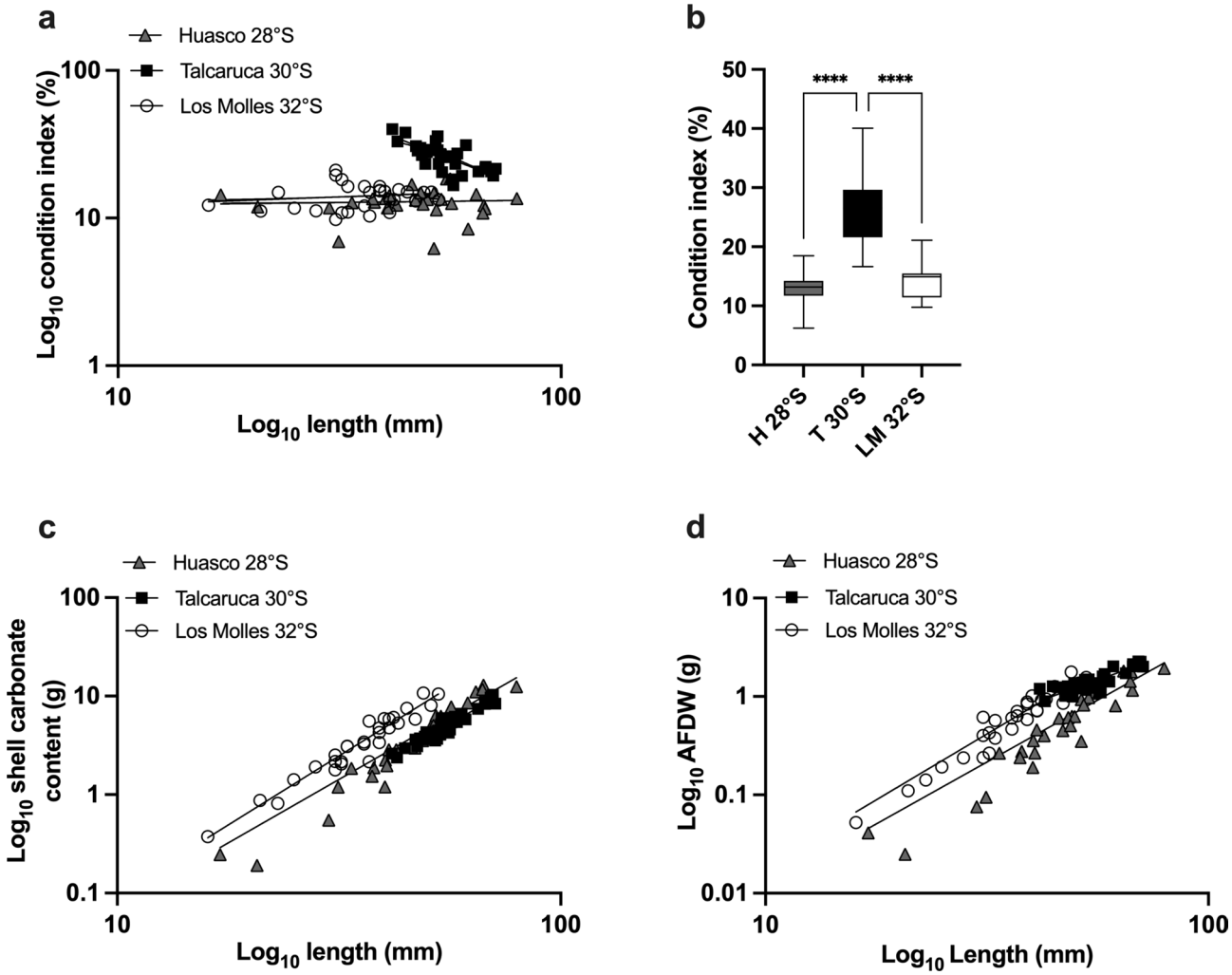

Fig. 2. Carbonate content-related parameters in three *Chiton granosus* populations across the biogeographical break in central north Chile. (**a**) Simple linear regressions (lines) of length and condition index (CI: dry biomass/ shell mass × 100). (**b**) Boxplots illustrating the range of CI values in the three populations (min to max). Asterisks indicate significant differences according to a Kruskall-Wallis and Dunn´s multiple comparison test ($p < 0.001$). (**c**) Simple linear regressions (lines) of length and shell carbonate content. (**d**) Simple linear regressions (lines) of length and Ash Free Dry Weight (AFDW). In panels (**a**), (**c**), and (**d**), the axes were $\log_{10}$ transformed, with each dot representing one organism, and the linear regressions were calculated on the $\log_{10}$ transformed data. Data from the different sites are represented as follows: white for Los Molles (LM), black for Talcaruca (T), and grey for Huasco (H).

obtained from individuals in Talcaruca exhibited lower dispersion, with individuals generally being larger and having higher AFDW levels compared to individuals from the other locations (Fig. 2d).

Abundance and physiological performance patterns

The abundance of individuals in each population was measured during different seasons from winter 2015 to autumn 2018 (Fig. 3). A grouped distribution was observed in all populations, with most quadrats having zero individuals and others showing high abundance. According to a two-way ANOVA, the locality effect was significant ($F_{2,21} = 7.728$, $P < 0.001$), and the interaction between locality and season was also significant ($F_{12,21} = 37.94$, $P = 0.013$). The maximal abundance of *C. granosus* individuals in a quadrat was observed in Talcaruca (164 ind./m^2), while the quadrat with the highest abundance in Huasco had 36 ind./m^2 and 144 ind./m^2 in Los Molles (Fig. 3). When comparing abundances by grouping the data seasonally, the average abundance per m^2 was lower in Talcaruca (7.43 ind./m^2) and Los Molles (5.88 ind./m^2) than in Huasco (11.04 ind./m^2). Notably, Talcaruca displayed the highest seasonal variation (SD = 5.54), while Huasco exhibited the lowest variation (SD = 4.30) (Fig. 3).

The metabolic rate was measured in individuals collected during the spring–summer season in the three populations (Fig. 4). Individuals from Talcaruca exhibited a significantly higher metabolic rate, surpassing those from Huasco by 141% ± 50 ($P = 0.0007$) and those from Los Molles by 322% ± 174 ($P < 0.001$) (Fig. 4).

The interaction between cardiac activity, as an indicator of physiological performance among chiton populations, and experimental temperatures followed the expected non-linear pattern, revealing the typical left-skewed shape of the TPC (best-fitted models in Table 3 and Fig. 5). The lowest heart rate values were observed at the extreme experimental temperatures (i.e., 2 and 38°C) for the three populations (Fig. 5). All three locations showed peak heart rate (i.e., T_{opt}) at similar temperatures: 27.36, 27.43, 27.27 °C for Huasco, Talcaruca, and Los Molles, respectively (Table 3). The thermal tolerance range of *C. granosus* exhibited the highest mean value for CT_{max} among individuals from Talcaruca (37.37 ± 2.24°C), followed by those from Huasco (36.88°C ± 2.71°C), and Los Molles (34.81°C ± 5.29) (Table 4) (Kruskal–Wallis ANOVA H test = 1.287; $P = 0.5254$) (Fig. 5). The critical minimum temperature (CT_{min}) significantly differed among chitons from the study sites. The lowest CT_{min} was recorded in Talcaruca (1.38 ± 0.77°C), while there was no significant difference between Los Molles and Huasco (Fig. 5 and Table 4). Furthermore, Warming Tolerance (WT), which provides an approximate average of the environmental warming that an ectothermic organism can withstand before reaching a lethal limit, showed the highest mean value in individuals from Talcaruca (20.53 ± 2.24°C), followed by those from Los Molles (18.58 ± 5.29°C) and then Huasco (18.15 ± 2.71°C) (Table 4) (Kruskal–Wallis ANOVA H test = 7.556; $P < 0.005$). The performance level of individuals at their optimal temperature (maximum performance μ_{max}) was higher in those from Los Molles (45.00 ± 13.43 beats per minute), followed by organisms from Talcaruca (44.87 ± 7.82 beats per minute), and then those from Huasco (40.85 ± 14.56 beats per minute) (Table 4), with no statistically significant differences (Kruskal–Wallis ANOVA H test = 0.2292; $P = 0.8917$) in μ_{max} between chitons of the three locations. The thermal breadth (T_{br}) of *C. granosus* was greater in organisms from the Talcaruca locality (22.45 ± 4.12 °C), followed by those from Los Molles (21.33 ± 3.72 °C), and then those from Huasco (17.83 ± 6.09°C) (Table 4) (Kruskal–Wallis ANOVA H test = 4.543; $P = 0.1031$).

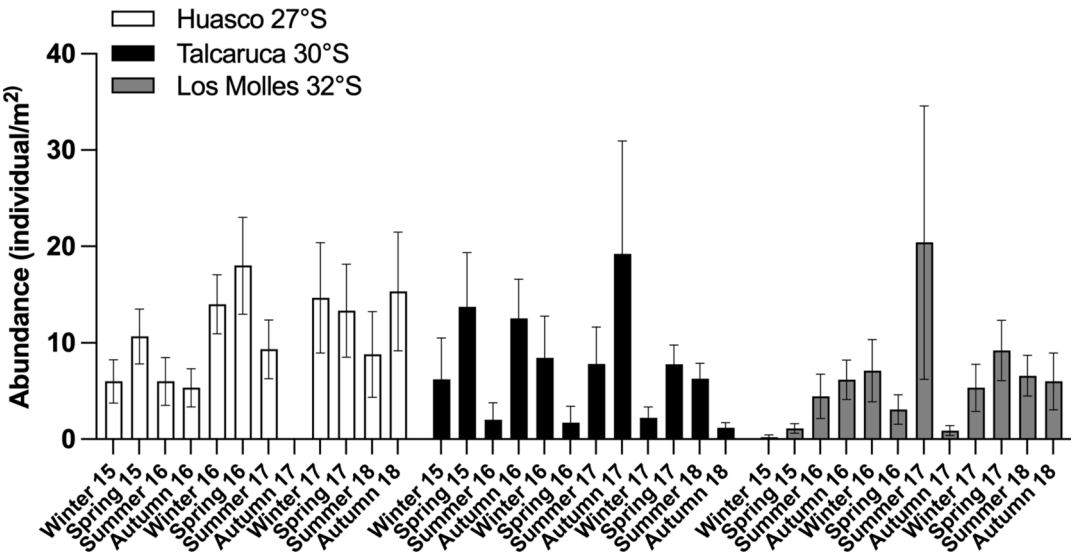

Fig. 3. Population abundance of *Chiton granosus* across the biogeographical break in central north Chile. Individual counts per square meter in Huasco (white bars), Talcaruca (black bars), and Los Molles (grey bars). Abundances were recorded across multiple seasons from winter 2015 to autumn 2018. Each bar corresponds to the average abundance ± standard error.

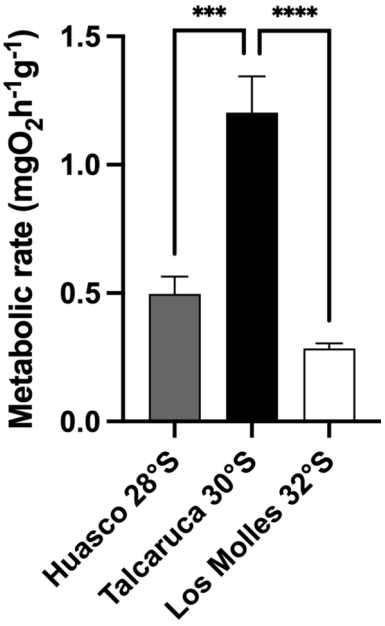

Fig. 4. Metabolic rate of *Chiton granosus* individuals form three populations of the biogeographical break in central north Chile. Bars represent the mean ± SEM of the metabolic rates of Individuals from Huasco (gray, n = 21), Talcaruca (black, n = 28), and Los Molles (white, n = 29). Asterisks indicate significant differences according to Kruskall-Wallis and Dunn´s multiple comparison tests (***$P < 0.001$, ****$P < 0.0001$).

Population	Function	K	r^2	AIC	λ_i	w_i
Huasco	**Weibull**	**4**	**0.44**	**24.57**	**−0.08**	**−1.81**
	Gaussian	3	0.37	28.31	0.09	0.41
	Lorentzian	3	0.22	29.72	0.21	0.49
Talcaruca	Weibull	5	0.33	78.82	−5.45	0.03
	Gaussian	**3**	**0.61**	**64.11**	**−5.71**	**0.65**
	Lorentzian	3	0.30	70.42	−6.94	0.53
Los Molles	Weibull	5	0.26	108.04	−7.83	0.31
	Gaussian	**3**	**0.57**	**91.71**	**−6.01**	**0.58**
	Lorentzian	3	0.38	94.55	−7.73	0.26

Table 3. Comparison of functions used to describe the thermal performance curves of *Chiton granosus* in three populations across upwelling center of Punta Lengua de Vaca, using Akaike's information criterion (AIC). The function with the lowest AIC is the one that best describes the data K, number of parameters in the function; λ_i, difference between a given model's AIC and the lowest AIC; w_i, Akaike weight. Models in boldface were selected for analyses.

Discussion

The environmental characterization of our study sites indicated that the Talcaruca area, located on the PLV headland upwelling center and the location of the biogeographic break between the Peruvian Province and the Transition zone, was persistently exposed to upwelled waters during our three-year study period. Seawater temperature values at the shore were lower and more variable compared to the two study sites located north and southward of the upwelling center. Similarly, carbonate system parameters differed markedly. While Huasco and Los Molles showed pH values within the current average ocean value (i.e., pH = 8.1[39,50]), Talcaruca presented values 0.2 units lower than the current coastal ocean average. The abrupt change in pH and temperature recorded in the Talcaruca locality was consistent with recent descriptions[51,52], which indicated that the area is characterized by a strong and semi-permanent upwelling regime. The presence of recently upwelled water was also supported by the high pCO_2 and DIC levels, which were consistent with the characteristics of deeper waters reaching the shore[8,53]. Moreover, the synoptic decorrelation scale at Talcaruca agreed with observations from records obtained at a moored buoy in the nearby Tongoy Bay documenting intense upwelling conditions nearshore[54]. The oceanographic conditions at our study site are associated with an eastern-boundary upwelling region, the Humboldt upwelling system, and occur along the western United States, South Africa, and the Iberian Peninsula[9]. It is predicted that these upwelling areas will be heavily impacted by progressive ocean acidification and climate

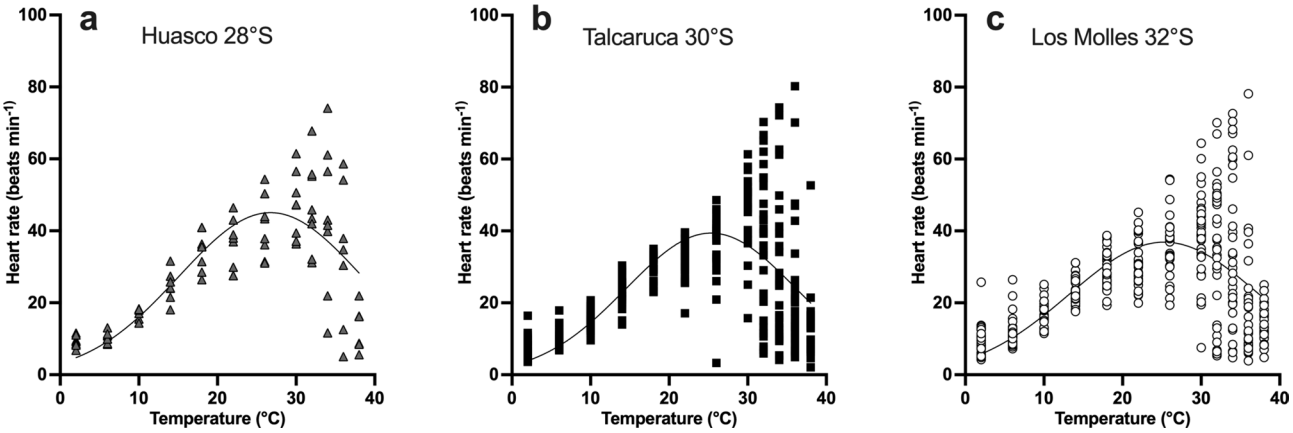

Fig. 5. Thermal performance curves of *Chiton granosus* across the biogeographical break in Central North Chile. Each dot represents the heart rate (beats/min) of an individual from Huasco (**a**, grey triangles), Talcaruca (**b**, black squares), and Los Molles (**c**, empty circles) at a specific temperature. A Gaussian curve was fitted to each dataset using nonlinear regression.

Population	CT_{min} (°C)	CT_{max} (°C)	T_{opt} (°C)	μ_{max}	WT (°C)	T_{br} (°C)
Huasco	2.50 ± 0.61**a**	36.88 ± 2.71	27.36 ± 2.70	40.85 ± 14.56	18.15 ± 2.71**a**	17.83 ± 6.08
Talcaruca	1.38 ± 0.77**b**	37.36 ± 2.24	27.43 ± 2.85	44.87 ± 7.82	20.53 ± 2.24**b**	22.45 ± 4.12
Los Molles	2.02 ± 0.20**a**	34.81 ± 5.29	27.27 ± 5.02	45.00 ± 13.43	18.58 ± 5.29**a**	21.33 ± 3.72
Statistical analyses						
Kruskal Wallis statistics	15.35	1.287	0.8909	0.2292	7.556	4.543
Number of values (total)	43	43	43	43	43	42
p-value*	**< 0.005**	0.5254	1.287	0.8917	**< 0.005**	0.1031

Table 4. Parameters of thermal performance curves in three populations of the chiton *Chiton granosus.* The table shows the estimated parameters with associated standard error (CT_{min}: Critical Thermal Minimum; $CT_{max:}$ Critical Thermal Maximum; T_{opt}: Optimal Temperature; μ_{max}: Heart Beat Maximum; WT: Warming Tolerance; T_{br}: Thermal Breadth). *Different letters indicate significant differences in the same parameter among the populations, as determined by Dunn's Multiple Comparison Test.

change[12,13,55]. It should be mentioned that a value 0.2 units lower on the pH scale implies a 45% increase in ocean acidity since the pH scale is logarithmic[56]. Additionally, as carbonate system parameters were higher in Talcaruca (i.e., DIC, CO_3^{2-}, pCO_2, Ω), some values were near corrosive levels for calcifying invertebrates[40]. The carbonate system parameters are closely related to the physiological tolerances of species and are considered limiting factors for the geographic distribution in ectothermic organisms through their influence on vital processes[32,38,57]. Changing patterns of environmental variation encompassed by the different biogeographic regions that occur along the vast latitudinal expanse of the Chilean coast implies that coastal organisms deploy different strategies of physiological adaptation[28,31,58], morphological changes[31,38,59], and behavioral responses[27,38,60] to thrive along their geographic range. Environmental variability can manifest gradually along environmental gradients, such as latitudinal clines, or abruptly at biogeographical breaks, where phenotypic traits can also change suddenly[31,61,62]. Therefore, phenotypic plasticity plays an important role in organisms with broad latitudinal distributions, enabling them to cope with significant environmental variability through physiological and morphological changes[32,34,63].

Mollusks belonging to the class *Polyplacophora*, commonly known as chitons, have earned the moniker "live fossils" due to their body plan remaining largely unchanged for over 300 million years. Although there are fossils from the early Paleozoic era, the diversity of chitons did not undergo a significant increase until the Cretaceous period[64]. These exclusively marine organisms inhabit intertidal habitats worldwide. The plates constituting their shells consist of two distinct layers: an outer surface enriched with organic content and an underlying calcareous layer. A thin periostracum may cover the plates[65]. Specifically, in several chitons' species, the mineral component (97–98% by weight) is aragonite, and its organic matrix (2–3% by weight) consists of highly glycosylated proteins[65]. X-ray diffraction and scanning electron microscopy show that the organic matrix fibers are aligned, morphologically and crystallographically, with the prismatic aragonite crystals[66]. Individuals of *C. granosus* from Los Molles showed the highest values of inorganic matter content in their shells per size range, followed by their conspecific from Huasco and Talcaruca. This spatial pattern of organic matter content is similar to what has been recorded in other calcifying organisms inhabiting areas with variable pCO_2 levels[38,67]. The observed values could be attributed to the pH fluctuations noted in the PLV zone. As several authors suggested, a decrease in pH could reduce the availability of carbonate ions, leading to surface waters becoming

undersaturated with respect to the aragonite mineral phase ($\Omega_{arag} < 1$)[39,50], a vital condition for shell building and calcification[40,68]. The undersaturation could lead to increased shell dissolution, as demonstrated by the high erosion index on shell surfaces reported at Talcaruca[69]. This is similar to what has been demonstrated in some mollusks and corals[70], as well as in some crustaceans like *Callinectes sapidus* Rathburn, 1896, *Penaeus plebejus* (Hess, 1865), and *Homarus americanus* (Milne-Edwards 1837), which can enhance their calcification capacity at high pCO_2 levels[67]. Some authors[40] suggest that this process can occur by using calcium bicarbonate (HCO_3^-) directly for calcification or by converting calcium bicarbonate into calcite ($CaCO_3$) through an internal proton regulation mechanism. Other studies suggest that tissues and external organic layers protect against corrosive waters, limiting the dissolution of calcareous structures[70,71]. *C. granosus* is a polyplacophoran with a very thin periostracum composed of sclerotized proteins capable of protecting the shell from corrosion in acidic waters[71]. It was recently demonstrated that juveniles of the gastropod *Conchocelepas concholepas* (Bruguière, 1789) favor the precipitation of calcite – a less soluble form of calcium carbonate – in their shells in place of aragonite – more sensitive to dissolution – as pH decreases[59]. When calcification increases to compensate for shell erosion under high pCO_2, it is followed by an increase in energy costs compromising other vital processes[72], such as metabolism[59,62,73], as we observed in Talcaruca (see Fig. 4). In addition to environmentally-induced shell dissolution, recent studies indicate additional challenges, such as infestation by photoautotrophic euendoliths, which may have significant impacts on calcifying organisms inhabiting coastal habitats[74].

Marine organisms continuously exposed to an acidic environment consume oxygen at higher rates, in contrast to populations experiencing regular periods of hypercapnia[36,38,63,73]. Similarly, we observed increased oxygen consumption in specimens of *C. granosus* from the Talcaruca locality. The pattern likely follows the elevated variability in pH and ambient temperature at the site and the high metabolic rates associated with the energy cost of maintaining homeostasis[32,60,75]. For example, Lardies et al. (2014) demonstrated geographic variation in the metabolic response of *C. concholepas* due to increased phenotypic plasticity in populations inhabiting naturally acidified areas (e.g., estuaries). The same trend was observed for other gastropods at Talcaruca[32,38]. The spatial pattern across these different gastropods likely reflects local adaptation. However, chitons exhibit species-specific metabolic adaptations to environmental pCO_2 conditions[76]. Little is known about the mechanisms supporting physiological compensation processes in chitons[77]. The group has experienced little change across different climate change events over geological scales, suggesting that they may deploy diverse physiological responses to the current anthropogenic climate change[76]. We observed a high metabolic rate and condition index in *C. granosus* at the biogeographic break of Talcaruca, which is likely related to the high variability in temperature and carbonate systems in the environment. This suggests that organisms in Talcaruca would show greater signs of phenotypic plasticity, given the wide environmental variability[31,34,61,78]. Assessing the physiological responses of organisms to ongoing ocean acidification and global warming will require us to integrate the geographical variability among populations to multiple stressors[32,63,79].

Upwelling-driven biogeographic breaks also influence patterns of community structure in association with patterns of oceanographic variability[42,80,81]. Greater temporal variability in *C. granosus* abundance at Talcaruca may be driven by high mortality rates or decreased growth rates during critical ontogenetic stages in association with the high metabolic cost of calcification[73,82]. On the other hand, higher densities and higher biomass (i.e., AFDW) could be directly related to the greater abundance of food (i.e., algae) at Talcaruca following high algal abundance and growth rates associated with coastal upwelling. The highest metabolic rates and the thinnest shells were observed in Talcaruca individuals. The trade-off between curtailed calcification and increased biomass suggests that energy was allocated to different metabolic processes; calcification is energetically costly[83,84] and metabolic cost was higher at Talcaruca (see Fig. 4).

Variations in thermal performance result from physiological adaptation to a specific thermal environmental condition[85,86]. These adaptations occur because ectothermic species use phenotypic plasticity to compensate for drastic environmental changes[78], which can reveal different patterns of thermal sensitivity and tolerance along a latitudinal gradient[33,62,87]. In *C. granosus*, we observed higher mean values for the maximum and minimum critical temperature (CT_{max}; CT_{min}) in the Talcaruca locality compared to the Huasco and Los Molles localities, while we did not detect differences in the optimal temperature (T_{opt}) among the three populations. Additionally, the thermal range was greater in individuals from Talcaruca. The spatial pattern suggests that the greater plasticity in thermal response follows the rapidly changing environmental conditions by individuals experience in Talcaruca. Populations residing in areas characterized by heterogeneous environments, yet relatively predictable environmental conditions, may demonstrate diminished plasticity[88]. Temperature decorrelation patterns in our multiyear records indicate that the site at the biogeographic break experiences less predictable environmental conditions compared to the sites outside this area. Additionally, this location exhibited the largest range of variability among the three localities, including high pCO_2 values, which can have physiological effects on the organisms in addition to ambient temperature[30,38]. The challenging environmental conditions at Talcaruca are fully consistent with the high values of standard metabolism we observed for individuals from the locality; cardiac output tends to be almost proportional to an individual's metabolic rate[89]. Populations experiencing more variable environmental conditions exhibit a wider physiological tolerance range than populations inhabiting more stable environments[32,78,90].

Future studies will need to partition the significance of the different stressors in eliciting plastic responses[91,92]. pH and temperature are not the only factors determining the physiological performance of organisms in upwelling systems. Identifying the role of other co-varying stressors, such as oxygen, salinity, carbonate system parameters, or nutrients, will be necessary to understand the effects of upwelling intensification on the geographic distribution of coastal organisms[11,37]. Physiological adaptability, especially to temperature, allows species with wide geographical distributions to span biogeographic barriers (e.g., PLV). Examples along the coast of Chile include the intertidal zone species *Acanthopleura equinata* (Barnes, 1824), *Scurria araucana* (A. d'Orbigny, 1839), *Petrolisthes laevigatus* (Guerin, 1835), *Jehlius cirratus* (Darwin, 1854) and *Chiton granosus*[32–34,93]. Global climate

models predict important environmental changes in coastal regions such as the South East Pacific, driven by the increase in sea surface temperatures and the increase in the intensity and duration of upwelling events in the coming decades[12,94–96]. Our results suggest that a trend similar to the "simplification not tropicalization" observed in other coastal ecosystems—where biodiversity decreases and a few resilient species dominate due to changing conditions—may also occur in upwelling ecosystems[97]. The winners and losers under ongoing climate change will likely be species with broad geographical distributions and a degree of phenotypic plasticity, enabling them to tolerate new environmental conditions under highly variable regimes.

Methods

Study sites and oceanographic conditions along the biogeographic break

Individuals of *C. granosus* (n = 70 per site, 40 for Metabolic Rate (MR) and Thermal Performance Curve (TPC), and 30–35 for estimation of biomass and shell carbonate production) were collected haphazardly by hand during low tide in the mid-intertidal zone during austral spring when upwelling activity is at its maxima in the region[98]. We selected individuals from three locations that straddle the 30°S coastal biogeographic break[38]. The northern location (Huasco, 28°41'S and 71°19'W) site is inside a region of weak non-seasonal upwelling, whereas the southern location (Los Molles, 32°24´S and 71°52´W) is within a region of seasonal upwelling[42,99,100]. Both locations represent our control locations. Our upwelling site, Talcaruca (30°48'S and 71°52'W), experiences a year-round upwelling regime[8,98] (see Fig. 1). In this way, our study sites have contrasting conditions of pH and SST[11,38,51] (Table 2 and Fig. 1).

In situ water temperature was monitored using Onset Hobo temperature loggers, which were housed inside PVC pipes embedded into concrete slabs anchored to the shore with stainless steel bolts and chains. The thermometers were positioned at a depth of at least 1 m below the low tide and monitored every two or three months. Temperature readings were recorded at sampling frequencies ranging from 10 to 30 min. Data for the three study sites are part of a long-term observational study and have been monitored for periods ranging from 8 to 17 years overlapping with the results of this study. Full details of the methods are provided in[52,101]. Using these long-term datasets, we interpolated the high-frequency records to daily values and calculated the annual cycle using the long-term daily mean smoothed with a 90-day (seasonal) running-mean filter. Using the long-term annual cycle, we removed seasonal variability, estimated the standardized daily anomalies, and used the full record to calculate the autocorrelation function over a 15-day lag[102]. Using the resulting autocorrelation function, we examined the degree of exposure to coastal upwelling and patterns of oceanographic variability at the rocky shore of each study site[103].

To characterize carbonate system parameters at each site, discrete water samples were taken (n = 20 in each site) over a period of two years. For pH measurements (total scale), two water samples were gathered and analyzed within 60 min of collection. The analysis was conducted using a Metrohm 826 pHMobile Meter© connected to a combined electrode (double junction), calibrated with TRIS buffers (pH = 8.089) at 25 °C with the aid of a thermo-regulable water bath. To analyze total alkalinity (AT), discrete water samples were collected in borosilicate glass bottles (Corning 500-mL). These samples were treated with mercuric chloride (0.2 cm^3 of a 50% saturated solution) and sealed with Apiezon® L grease for transportation to the laboratory. The samples were stored for no more than 2 months under cool, dark conditions until analysis. For AT measurement, three to five seawater subsamples from each bottle were used, and the analysis was carried out using automated potentiometric titration[104]. The partial pressure of CO_2 (pCO_2) and saturation states (Ω) for calcite and aragonite were estimated based on averaged values of pH_T, AT, and SST using the CO2SYS software[105].

Animal abundance patterns, collection and maintenance

To estimate the patterns of local abundance, quadrats (25 × 25 cm; n = 6 to n = 36 per site at mid and low tidal heights) were deployed in two transects parallel to the coastline from 2015 to 2018. In the Autumn of 2017, it was not possible to sample the abundance of chitons at the Huasco site due to surge conditions. During the spring and summer of 2016 and 2017, individuals of *C. granosus* were collected from each study site and transported in refrigerated containers. They were covered with wet cellulose sponge cloths soaked in seawater and then taken to the laboratory at Adolfo Ibañez University in Santiago. Animals were acclimated for two weeks in a common garden aquarium to assess their physiological compensation across the biogeographic break. They were provided with ad libitum food, including stones covered with *Ulva spp*. And coralline algae, which were collected at each site and transported to the laboratory as described above. The containers were constantly aerated with artificial seawater (InstantOcean®) maintained at 14 ± 1 °C using a temperature controller device (SunSun®), with a pH of 8.0 ± 0.1 and a salinity of 33 ± 1 PSU. These averaged values of the Chilean coast were monitored using a pH meter (Metrohm model 826) and a salinometer (Salt6 + , Oakton; accuracy: ± 0.1 PSU), respectively. A light regime of 12:12 was used. Each chiton was individualized using a numerical and colored bee mark (beeworks©) glued on the second shell plate. Chitons were characterized in terms of Total Length (TL) (i.e., from anterior to posterior mantle girdle) with a digital caliper (Litz®) and wet weight (WW) with an analytical balance (Shimadzu, model AUX220).

Oxygen consumption measurements

Measurements of oxygen consumption were made for individual specimens of *C. granosus* from Huasco (n = 25), Talcaruca (n = 31) and Los Molles (n = 33) using fiber optic oxygen sensors (Precision Sensing, GmbH, Germany) connected to a PreSens Oxy-4 mini® respirometer. Animals were assayed inside hermetic glass chambers (Schott) of 113 mL connected to the sensor and filled up with UV-filtered water. For oxygen consumption rates measurements, individuals were previously starved for 24 h at pH 8.0 ± 0.1, 33 ± 1 PSU, and 14 °C water conditions and spring natural photoperiod (14D:10N). The temperature was stabilized using a recirculating water

bath (BOYU, Model L075). Sensors were previously calibrated with saturated Na_2SO_3 solution and aerated sea water, to estimate 0% and 100% oxygen, respectively. Sensors measured water oxygen levels every 15 s over about 60 min. To obtain multiple estimates, the first 10 and last 5 min of measurements were discarded to mitigate potential disturbances associated with animal stress caused by handling. The results of mean oxygen rates between populations were expressed as per gram of animal wet weight (i.e., $mgO_2L^{-1}\ h^{-1}\ g^{-1}$).

Biomass and shell carbonates content

We measured the biomass and shell carbonate content on animals from Huasco (n = 32), Talcaruca (n = 41) and Los Molles (n = 31). After recording the total length (mm) of chitons we dissected the shell plates and soft tissues of each individual and separated them in foil packages previously weighed and numbered. We then dried the plates and soft tissues at 80 °C in a LabTech™ model LDO-080F oven for 72 h and weighed them to obtain dry tissue weight. Afterwards, all dry packages were calcinated into a Vulcan model A-550 muffle furnace for 4 h at 450 °C. Ash-free Dry Weight (AFDW, g) was calculated by subtracting the inorganic ashes from dry tissue weight. Shell weights after calcination were regarded as a proxy of the carbonate content of the shells[82]. We also computed the condition index (CI) for each chiton, expressed as the ratio of dry tissue weight to dry shell weight (× 100)[38].

Thermal performance curves (TPC)

Thermal effects on physiological performances were estimated for individuals from Huasco (n = 9), Los Molles (n = 22), and Talcaruca (n = 13) using an electric heart sensor on the seventh plate (heart location) connected to an Oscilloscope (TiePie engineering, model HS4) to estimate the Heart Rate (HR, cardiac activity)[31]. Animals were immobilized with adhesive tape on a wet plate and introduced into a thermoregulated chamber (JeioTech, model RW-2025). Electric impulses were registered as an electrocardiogram by the program Multi-Channel Oscilloscope v1.31.2.0 (TiePie engineering). Measurements of HR were made for each organism at temperatures of 2, 6, 10, 14, 18, 22, 26, 32, 34, 36, and 38 °C. These temperature choices were supported by prior pilot experiments on the thermal performance curve in *C. granosus*. The first measurement started at 14 °C, and then the temperatures were decreased to 10, 6, 4, and 2 °C. Subsequently, chitons were brought to a higher temperature starting at 18 °C and gradually increasing to 22, 26, 30, 32, 34, 36 up to 38 °C, and returned to the aquarium. At initial temperatures (i.e., 14 °C and 18 °C) acclimation lasted 30 min to avoid stress caused by manipulations. After 10 min of data recorded the temperature was changed, waiting 20 min for the organism to adjust. An estimate of the TPC was then generated to calculate the heart rate mean for each experimental temperature and site. Statistical package TableCurve2D 5.01 (SYSTAT Software Inc.) was used to fit the curve. Several functions that could describe the chiton's heart rate, as a function of temperature, were compared using the Akaike Information Criterion (i.e., AIC)[106] corrected by small sample size. The optimal temperature (T_{opt}) was obtained from the maximum heart rates at all experimental temperatures, by site. Critical temperature values (CT_{max} and CT_{min}) were generated as the intersection points of the performance curve with the temperature axis (frequency = 0). The thermal amplitude (T_{br}) for each population was calculated by means of the heart rates, at each experimental temperature using the following Eq. [107]:

$$\mathrm{Tbr} = \sqrt{\sum_{i=0}^{N}\left[\frac{\mu_i\left(T_i - T_{opt}\right)}{\mu_{max}}\right]^2}$$

where N represents the number of temperatures, and μ_i is the average of heart rate at temperature T_i. We also estimated Warming Tolerance (WT) of each population following[90]:

$$\mathrm{WT} = \mathrm{CT_{max}} - \mathrm{T_{hab}}$$

Statistical analyses

All data analyses were performed using GraphPad Prism version 10.0.3 for macOS, GraphPad Software, San Diego, California USA or MatLab R2014B. We performed a one-way multivariate analysis of variance (MANOVA) using Wilk´s λ as a statistical test and using Dunnett C as a post hoc test, including all carbonate system parameters to estimate differences in environmental conditions among sites. Furthermore, we used one-way ANOVA to estimate differences in salinity, pH, and alkalinity for mean conditions at the three study locations. A simple linear regression was used to describe the relationship between the total length (L) and the condition index (CI) of chitons from each population. The same was performed to analyze the shell carbonate content and the ash-free dry weight (AFDW) as function of total length. In all cases, data from at least 29 individuals per site were compared. Variables analysed in linear regressions were transformed using $\log_{10}$-$\log_{10}$. The assumptions for linear regression of the normality and linearity were checked by means of Kolgomorov-Smirnov test and residual vs fitted plot, respectively. The slopes were then compared between each population using an ANCOVA.

We used a nonparametric Kruskal–Wallis analysis and Dunn's Multiple Comparisons Test to compare the condition index (n = 26 to 31 individuals per population), metabolic rate (n = 21 to 29 individuals per population), and TPC parameters (n = 9 to 21 individuals per population) because the underlying data did not follow a normal distribution. We estimated a TPC for each chiton at each site, determined 7 parameters for each individual, and then applied the Kruskal–Wallis Test. Finally, a two-way analysis of variance (ANOVA) was performed to determine the effects of source population and season on chitons abundance, followed by Tukey's a posteriori HSD tests. Prior to all statistical analyses, the data were tested for normality and homogeneity of variance using the Kolmogorov–Smirnov and Levene tests, respectively.

Data availability

All data that support the findings of this study are included within the article (and any supplementary information files).

Received: 30 May 2024; Accepted: 9 September 2024
Published online: 13 September 2024

References

1. Doney, S. C. *et al.* Climate change impacts on marine ecosystems. *Ann. Rev. Mar. Sci.* **4**, 11–37. https://doi.org/10.1146/annurev-marine-041911-111611 (2012).
2. Keeling, R. F., Körtzinger, A. & Gruber, N. Ocean deoxygenation in a warming world. *Ann. Rev. Mar. Sci.* **2**, 199–229. https://doi.org/10.1146/annurev.marine.010908.163855 (2010).
3. Gattuso, J.-P. *et al.* Contrasting futures for ocean and society from different anthropogenic CO_2 emissions scenarios. *Science* **349**, 6243. https://doi.org/10.1126/science.aac4722 (2015).
4. Poloczanska, E. S. *et al.* Global imprint of climate change on marine life. *Nat. Clim. Change* **3**, 919–925. https://doi.org/10.1038/nclimate1958 (2013).
5. Halpern, B. S. *et al.* Drivers and implications of change in global ocean health over the past five years. *PLOS ONE* **12**, e0178267. https://doi.org/10.1371/journal.pone.0178267 (2017).
6. Bednaršek, N. *et al.* Niño-related thermal stress coupled with upwelling-related ocean acidification negatively impacts cellular to population-level responses in pteropods along the California Current System with implications for increased bioenergetic costs. *Front. Mar. Sci.* **4**, 486. https://doi.org/10.3389/fmars.2018.00486 (2018).
7. Breitburg, D. *et al.* Declining oxygen in the global ocean and coastal waters. *Science* **359**(6371), eaam7240. https://doi.org/10.1126/science.aam7240 (2018).
8. Torres, R. *et al.* Air-sea CO_2 fluxes along the coast of Chile: From CO_2 outgassing in central northern upwelling waters to CO_2 uptake in southern Patagonian fjords. *J. Geoph. Res.* **116**, C09006. https://doi.org/10.1029/2010JC006344 (2011).
9. Gruber, N. *et al.* Rapid progression of Ocean acidification in the California current system. *Science* **337**, 220–223. https://doi.org/10.1126/science.1216773 (2012).
10. Hauri, C., Gruber, N., McDonnell, A. M. & Vogt, M. The intensity, duration, and severity of low aragonite saturation state events on the California continental shelf. *Geoph. Res. Lett.* **40**, 3424–3428. https://doi.org/10.1002/grl.50618 (2013).
11. Vargas, C. A. *et al.* Species-specific responses to ocean acidification should account for local adaptation and adaptive plasticity. *Nat. Ecol. Evol.* **1**, 0084. https://doi.org/10.1038/s41559-017-0084 (2017).
12. Sydeman, W. J. *et al.* Climate change and wind intensification in coastal up-welling ecosystems. *Science* **345**, 77–80. https://doi.org/10.1126/science.1251635 (2014).
13. García-Reyes, M. *et al.* Under pressure: Climate change, upwelling, and Eastern Boundary upwelling ecosystems. *Front. Mar. Sci.* **2**, 1–10. https://doi.org/10.3389/fmars.2015.00109 (2015).
14. Rykaczewski, R. R. *et al.* Poleward displacement of coastal upwelling-favorable winds in the ocean's eastern boundary currents through the 21st century. *Geophys. Res. Lett.* **42**, 6424–6431. https://doi.org/10.1002/2015GL064694 (2015).
15. Pespeni, M. H., Chan, F., Menge, B. A. & Palumbi, S. R. Signs of adaptation to local pH conditions across an environmental mosaic in the California current ecosystem. *Integr. Comp. Biol.* **53**, 857–870. https://doi.org/10.1093/icb/ict094 (2013).
16. Gaitán-Espitia, J. D. *et al.* Spatio-temporal environmental variation mediates geographical differences in phenotypic responses to ocean acidification. *Biol. Lett.* **13**, 20160865. https://doi.org/10.1098/rsbl.2016.0865 (2017).
17. Gaitán-Espitia, J. D. *et al.* Geographical gradients in selection can reveal genetic constraints for evolutionary responses to ocean acidification. *Biol. Lett.* **13**, 20160784. https://doi.org/10.1098/rsbl.2016.0784 (2017).
18. Andersson, A. J. *et al.* Understanding ocean acidification impacts on organismal to ecological scales. *Oceanography* **28**(2), 16–27. https://doi.org/10.5670/oceanog.2015.27 (2015).
19. Benítez, S. *et al.* High pCO_2 levels affect metabolic rate, but not feeding behavior and fitness, of farmed giant mussel *Choromytilus chorus*. *Aquacult. Environ. Interact.* **10**, 267–278. https://doi.org/10.3354/aei00271 (2018).
20. Byrne, M. Impact of ocean warming and ocean acidification on marine invertebrates life history stages: Vulnerabilities and potential for persistence in a changing ocean. *Oceanogr. Mar. Biol.* **49**, 1–42. https://doi.org/10.1201/b11009 (2011).
21. Navarro, J. M. *et al.* Ocean warming and elevated carbon dioxide: Multiple stressor impacts on juvenile mussels from southern Chile. *ICES J. Mar. Sci.* **73**, 764–771. https://doi.org/10.1093/icesjms/fsv249 (2016).
22. Lardies, M. A. *et al.* Physiological and histopathological impacts of increased carbon dioxide and temperature on the scallops *Argopecten purpuratus* cultured under upwelling influences in northern Chile. *Aquaculture* **479**, 455–466. https://doi.org/10.1016/j.aquaculture.2017.06.008 (2017).
23. Parker, L. M., Ross, P. M. & O'Connor, W. A. Comparing the effect of elevated pCO_2 and temperature on the fertilization and early development of two species of oysters. *Mar. Biol.* **157**, 2435–2452. https://doi.org/10.1007/s00227-010-1508-3 (2010).
24. Duarte, C. *et al.* Combined effects of temperature and ocean acidification on the juvenile individuals of the mussel *Mytilus chilensis*. *J. Sea Res.* **85**, 308–314. https://doi.org/10.1016/j.seares.2013.06.002 (2014).
25. Duarte, C. *et al.* The energetic physiology of juvenile mussels, *Mytilus chilensis* (Hupe): the prevalent role of salinity under current and predicted pCO_2 scenarios. *Environ. Pollut.* **242**, 156–163. https://doi.org/10.1016/j.envpol.2018.06.053 (2018).
26. Dupont, S., Dorey, N., Stumpp, M., Melzner, F. & Thorndyke, M. Long-term and trans- life-cycle effects of exposure to ocean acidification in the green sea urchin *Strongylocentrotus droebachiensis*. *Mar. Biol.* **160**, 1835–1843. https://doi.org/10.1007/s00227-012-1921-x (2012).
27. Manríquez, P. H. *et al.* Ocean acidification affects predator avoidance behaviour but not prey detection in the early ontogeny of a keystone species. *Mar. Ecol. Prog. Ser.* **502**, 157–167. https://doi.org/10.3354/meps10703 (2014).
28. Lagos, N. A. *et al.* Effects of temperature and ocean acidification on shell characteristics of *Argopecten purpuratus*: implications for scallop aquaculture in an upwelling-influenced area. *Aquacult. Environ. Interact.* **8**, 357–370. https://doi.org/10.3354/aei00183 (2016).
29. Zippay, M. L. & Hofmann, G. E. Effect of pH on gene expression and thermal tolerance of early life history stages of red abalone (*Haliotis rufescens*). *J. Shellfish. Res.* **29**, 429–439. https://doi.org/10.2983/035.029.0220 (2010).
30 Lefevre, S. Are global warming and ocean acidification conspiring against marine ectotherms? A meta-analysis of the respiratory effects of elevated temperature, high CO_2 and their interaction. *Conserv. Physiol.* **4**, COW009. https://doi.org/10.1093/conphys/cow009 (2016).
31. Lardies, M. A., Caballero, P., Duarte, C. & Poupin, M. J. Geographical variation in phenotypic plasticity of intertidal sister limpet's species under ocean acidification scenarios. *Front. Mar. Sci.* **8**, 1–13. https://doi.org/10.3389/fmars.2021.647087 (2021).
32. Rodríguez-Romero, A., Gaitán-Espitía, J. D., Opitz, T. & Lardies, M. A. Heterogeneous environmental seascape across a biogeographic break influences the thermal physiology and tolerances to ocean acidification in an ecosystem engineer. *Divers. Distrib.* **28**, 1542–1553. https://doi.org/10.1111/ddi.13478 (2022).

33. Gaitán-Espitia, J. D. *et al.* Geographic variation in thermal physiological performance of the intertidal crab *Petrolisthes violaceus* along a latitudinal gradient. *J. Exp. Biol.* **217**, 4379–4386. https://doi.org/10.1242/jeb.108217 (2014).
34. Broitman, B. R. *et al.* Phenotypic plasticity is not a cline: Thermal physiology of an intertidal barnacle over 20° of latitude. *J. Anim. Ecol.* **90**, 1961–1972. https://doi.org/10.1111/1365-2656.13514 (2021).
35. Willmer, P., Stone, G. & Johnston, I. *Environmental physiology of animals* 2nd edn. (Blackwell, 2005).
36. Pörtner, H. O., Langenbuch, M. & Reipschläger, A. Biological impact of elevated ocean CO_2 concentrations: lessons from animal physiology and earth history. *J. Oceanography* **60**, 705–718 (2004).
37. Somero, G. N. *et al.* What changes in the carbonate system, oxygen, and temperature portend for the Northeastern Pacific Ocean: a physiological perspective. *Biosci.* **66**, 14–26. https://doi.org/10.1093/biosci/biv162 (2016).
38. Broitman, B. R., Aguilera, M. A., Lagos, N. A. & Lardies, M. A. Phenotypic plasticity at the edge: Contrasting population–level responses at the overlap of the leading and rear edges of the geographical distribution of two *Scurria* limpets. *J. Biogeogr.* **45**, 2314–2325. https://doi.org/10.1111/jbi.13406 (2018).
39. Orr, J. C. *et al.* Anthropogenic ocean acidification over the twenty-first century and its impact on calcifying organisms. *Nature* **437**, 681–686. https://doi.org/10.1038/nature04095 (2005).
40. Fabry, V., Seibel, B., Feely, R. & Orr, J. Impacts of ocean acidification on marine fauna and ecosystem processes. *ICES J. Mar. Sci.* **65**, 414–432. https://doi.org/10.1093/icesjms/fsn048 (2008).
41. Palmer, A. R. Growth in marine gastropods: A non-destructive technique for independently measuring shell and body weight. *Malacologia* **23**, 63–73 (1982).
42. Broitman, B. R., Navarrete, S., Smith, F. & Gaines, S. Geographic variation of southeastern Pacific intertidal communities. *Mar. Ecol. Prog. Ser.* **224**, 21–34 (2001).
43. Sanhueza, V. & Ibáñez, C. M. *Chiton granosus* Frembly, 1827 (Mollusca, Polyplacophora): antecedentes de la especie. *Amici Molluscarum* **24**, 23–28 (2016).
44. Hickman, C. S. Analysis of microstructural similarity: Lessons from the gastropod shell, radula, and sensory epithelium. *Proc. Mod. Microscopy/Scanning* **25**, 62–64 (2003).
45. Aguilera, M. A. & Navarrete, S. A. Effects of *Chiton granosus* (Frembly, 1827) and other molluscan grazers on algal succession in wave exposed mid-intertidal rocky shores of central Chile. *J. Exp. Mar. Biol. Ecol.* **349**, 84–98. https://doi.org/10.1016/j.jembe.2007.05.002 (2007).
46. Piersma, T. & Drent, J. Phenotypic flexibility and the evolution of organismal design. *Trends Ecol. Evol.* **18**, 228–233. https://doi.org/10.1016/S0169-5347(03)00036-3 (2003).
47. Sunday, J. M. *et al.* Thermal-safety margins and the necessity of thermoregulatory behavior across latitude and elevation. *Proc. Nat. Acad. Sci. USA* **111**, 5610–5615. https://doi.org/10.1073/pnas.1316145111 (2014).
48. Chevin, L. M., Lande, R. & Mace, G. M. Adaptation, plasticity, and extinction in a changing environment: towards a predictive theory. *PloS Biol* **8**, e1000357. https://doi.org/10.1371/journal.pbio.1000357 (2010).
49. Calosi, P., Wit, P. D., Thor, P. & Dupont, S. Will life find a way? Evolution of marine species under global change. *Evol. Appl.* **9**, 1035–1042. https://doi.org/10.1111/eva.12418 (2016).
50. IPCC. *Summary for policymakers*. In V. Masson-Delmotte, P. Zhai, H.-O. Pörtner, D. Roberts, J. Skea, P. R. Shukla, A. Pirani, W. Moufouma-Okia, C. Péan, R. Pidcock, S. Connors, J. B. R. Matthews, Y. Chen, X. Zhou, M. I. Gomis, E. Lonnoy, T. Maycock, M. Tignor, & T. Waterfield (Eds.), Global warming of 1.5°C. An IPCC Special Report on the impacts of global warming of 1.5°C above pre-industrial levels and related global greenhouse gas emission pathways, in the context of strengthening the global response to the threat of climate change, sustainable development, and efforts to eradicate poverty (pp. 1–24). IPCC (2018).
51. Aravena, G., Broitman, B. R. & Stenseth, N. C. Twelve years of change in coastal upwelling along the central-northern coast of Chile: spatially heterogeneous responses to climatic variability. *PloS One* **9**, e90276. https://doi.org/10.1371/journal.pone.0090276 (2014).
52. Tapia, F. J., Largier, J. L., Castillo, M., Wieters, E. A. & Navarrete, S. A. Latitudinal Discontinuity in Thermal Conditions along the Nearshore of Central-Northern Chile. *PloS ONE* **9**, e110841. https://doi.org/10.1371/journal.pone.0110841 (2014).
53. Torres, R. *et al.* Evaluation of a semi-automatic system for long-term seawater carbonate chemistry manipulation. *Rev. Chil. Hist. Nat.* **86**, 443–451. https://doi.org/10.4067/S0716-078X2013000400006 (2013).
54. Ramajo, L. *et al.* Upwelling intensity modulates the fitness and physiological performance of coastal species: Implications for the aquaculture of the scallop *Argopecten purpuratus* in the Humboldt Current System. *Sci. Total Environ.* **745**, 140949. https://doi.org/10.1016/j.scitotenv.2020.140949 (2020).
55. Lachkar, Z. Effects of upwelling increase on ocean acidification in the California and Canary Current systems. *Geoph. Res. Lett.* **41**, 90–95. https://doi.org/10.1002/2013GL058726 (2014).
56. Riebesell, U., Fabry, V. J., Hansson, L. & Gattuso, J.-P. *Guide to Best Practices for Ocean Acidification Research and Data Reporting* (Publications Office of the European Union, 2010).
57. Hofmann, G. E. & Todgham, A. E. Living in the now: physiological mechanisms to tolerate a rapidly changing environment. *Annu. Rev. Physiol.* **72**, 127–145. https://doi.org/10.1146/annurev-physiol-021909-135900 (2010).
58. Lardies, M. A., Muñoz, J. L., Paschke, K. A. & Bozinovic, F. Latitudinal variation in the aerial/aquatic ratio of oxygen consumption of a supratidal high rocky-shore crab. *Mar. Ecol.* **32**, 42–51. https://doi.org/10.1111/j.1439-0485.2010.00408.x (2011).
59. Ramajo, L., Rodriguez-Navarro, A., Duarte, C., Lardies, M. A. & Lagos, N. A. Shifts in shell mineralogy and metabolism of *Concholepas concholepas* juveniles along the Chilean coast. *Mar. Freshw. Res.* **66**, 1147–1157. https://doi.org/10.1071/MF14232 (2015).
60. Duarte, C. *et al.* Morphological, physiological and behavioral responses of an intertidal snail, *Acanthina monodon* (Pallas), to projected ocean acidification and cooling water conditions in upwelling ecosystems. *Env. Pollut.* **293**, 118481. https://doi.org/10.1016/j.envpol.2021.118481 (2022).
61. Barria, A. M., Lardies, M. A., Beckerman, A. P. & Bacigalupe, L. D. Latitude or biogeographic breaks? Determinants of phenotypic (co) variation in fitness-related traits in *Betaeus runcates* along the Chilean coast. *Mar. Biol.* **161**, 111–118. https://doi.org/10.1007/s00227-013-2319-0 (2014).
62. Barria, A. M., Bacigalupe, L. D., Lagos, N. A. & Lardies, M. A. Thermal physiological traits and plasticity of metabolism are sensitive to biogeographic breaks in a rock-pool marine shrimp. *J. Exp. Biol.* **221**, jeb181008. https://doi.org/10.1242/jeb.181008 (2018).
63. Lardies, M. A. *et al.* Differential response to ocean acidification in physiological traits of *Concholepas concholepas* populations. *J. Sea Res.* **90**, 127–134. https://doi.org/10.1016/j.seares.2014.03.010 (2014).
64. Vendrasco, M. J., Wood, T. E. & Runnegar, B. N. Articulated Palaeozoic fossil with 17 plates greatly expands disparity of early chitons. *Nature* **429**, 288–291. https://doi.org/10.1038/nature02548 (2004) (**PMID: 15152250**).
65. Peebles, B., Smith, A. M. & Spencer, H. G. Valve microstructure and phylomineralogy of New Zealand chitons. *J. Struct. Biol.* **197**, 250–259. https://doi.org/10.1016/j.jsb.2016.12.002 (2017).
66. Treves, K., Traub, W., Weiner, S. & Addadi, L. Aragonite formation in the chiton (Mollusca) girdle. *Helv. Chim. Acta* **86**, 1101–1112. https://doi.org/10.1002/hlca.200390096 (2003).
67. Ries, J. B., Cohen, A. L. & McCorkle, D. C. Marine species exhibit mixed responses to CO_2-induced ocean acidification. *Geology* **37**, 1131–1134. https://doi.org/10.1130/G30210A.1 (2009).

68. Figuerola, B. *et al.* A review and meta-analysis of potential Impacts of ocean acidification on marine calcifiers from the Southern Ocean. *Front. Mar. Sci.* **8**, 584445. https://doi.org/10.3389/fmars.2021.584445 (2021).
69. Fernández, C. *Desempeño fisiológico del molusco poliplacóforo intermareal Chiton granosus (Freembly, 1827) a lo largo de un quiebre biogeográfico en la costa de Chile*. Undergraduate Thesis Marine Biology Degree, Universidad de Valparaíso, Valparaíso, 74 pp. (2016).
70. Rodolfo-Metalpa, R. *et al.* Coral and mollusc resistance to ocean acidification adversely affected by warming. *Nat. Clim. Change* **1**, 308–312. https://doi.org/10.1038/nclimate1200 (2011).
71. Lagos, N. A. *et al.* Plasticity in organic composition maintains biomechanical performance in shells of juvenile scallops exposed to altered temperature and pH conditions. *Sci. Rep.* **11**, 24201. https://doi.org/10.1038/s41598-021-03532-0 (2021).
72. Telesca, L. *et al.* Biomineralization plasticity and environmental heterogeneity predict geographical resilience patterns of foundation species to future change. *Glob. Change Biol.* **25**, 4179–4193. https://doi.org/10.1111/gcb.14758 (2019).
73. Beniash, E., Ivanina, A., Lieb, N. S., Kurochkin, I. & Sokolova, I. M. Elevated level of carbon dioxide affects metabolism and shell formation in oysters *Crassostrea virginica*. *Mar. Ecol. Prog. Ser.* **419**, 95–108. https://doi.org/10.3354/meps08841 (2010).
74. Dievart, A. M. *et al.* Photoautotrophic euendoliths and their complex ecological effects in marine bioengineered ecosystems. *Diversity* **14**, 737. https://doi.org/10.3390/d14090737 (2022).
75 Arnold, K. E., Findlay, H. S., Spicer, J. I., Daniels, C. L. & Boothroyd, D. Effect of CO2-related acidification on aspects of the larval development of the European lobster, *Homarus gammarus* (L.). *Biogeosciences* **6**, 1747–1754 (2009).
76. Carey, N., Galkin, A., Henriksson, P., Richards, J. G. & Sigwart, J. D. Variation in oxygen consumption among 'living fossils' (Mollusca: Polyplacophora). *J. Mar. Biol. Ass. UK* **93**, 197–207. https://doi.org/10.1017/S0025315412000653 (2013).
77. Sigwart, J. D. & Carey, N. Grazing under experimental hypercapnia and elevated temperature does not affect the radula of a chiton (Mollusca, Polyplacophora, Lepidopleurida). *Mar. Environ. Res.* **102**, 73–77. https://doi.org/10.1016/j.marenvres.2014.05.004 (2014).
78. Naya, D. E., Catalan, T. P., Artacho, P., Gaitán-Espitía, J. D. & Nespolo, R. F. Exploring the functional association between physiological flexibility, climatic variability and geographical latitude: lesson from land snails. *Evol. Ecol. Res.* **13**, 647–659 (2011).
79. Lagos, M., Cáceres, C. W. & Lardies, M. A. Geographic variation in acid- base balance of the intertidal crustacean *Cyclograpsus cinereus* (Decapoda, Grapsidae) during air exposure. *J. Mar. Biol. Ass. UK* **94**, 159–165. https://doi.org/10.1017/S0025315413001264 (2013).
80. Fenberg, P. B., Menge, B. A., Raimondi, P. T. & Rivadeneira, M. M. Biogeographic structure of the northeastern Pacific rocky intertidal: the role of upwelling and dispersal to drive patterns. *Ecography* **38**, 83–95. https://doi.org/10.1111/ecog.00880 (2015).
81. Rose, J. M. *et al.* Biogeography of ocean acidification: Differential field performance of transplanted mussels to upwelling-driven variation in carbonate chemistry. *PLoS ONE* **15**, e0234075. https://doi.org/10.1371/journal.pone.0234075 (2020).
82. Ramajo, L. *et al.* Biomineralization changes with food supply confer juvenile scallops (*Argopecten purpuratus*) resistance to ocean acidification. *Glob. Change Biol.* **22**, 2025–2037. https://doi.org/10.1111/gcb.13179 (2016).
83. Palmer, A. R. Calcification in marine molluscs: how costly is it?. *Proc. Natl. Acad. Sci. USA* **89**, 1379–1382. https://doi.org/10.1073/pnas.89.4.137 (1992).
84. Waldbusser, G. G. *et al.* A developmental and energetic basis linking larval oyster shell formation to ocean acidification. *Geophys. Res. Lett.* **40**, 2171–2176. https://doi.org/10.1002/grl.50449 (2013).
85. Huey, R. B. & Kingsolver, J. G. Variation in universal temperature dependence of biological rates. *Proc. Natl. Acad. Sci. USA* **108**, 10377–10378. https://doi.org/10.1073/pnas.1107430108 (2011).
86. Gaitán-Espitía, J. D., Arias, M. B., Lardies, M. A. & Nespolo, R. F. Variation in thermal sensitivity and thermal tolerances in an invasive species across a climatic gradient: Lessons from the land snail *Cornu aspersum*. *PLoS ONE* **8**, e70662. https://doi.org/10.1371/journal.pone.0070662 (2013).
87. Bonebrake, T. C. & Deutsch, C. A. Climate heterogeneity modulates impact of warming on tropical insects. *Ecology* **93**, 449–455. https://doi.org/10.1890/11-1187.1 (2012).
88. Leung, C., Rescan, M., Grulois, D. & Chevin, M. Reduced phenotypic plasticity evolves in less predictable environments. *Ecol. Lett.* **23**, 1664–1672. https://doi.org/10.1111/ele.13598 (2020).
89. Bruning, A. *et al.* Energy metabolism, heart rate and physiological differentiation in the pulmonate gastropod *Cornu aspersum*. *J. Molluscan Stud.* **79**, 257–262. https://doi.org/10.1093/mollus/eyt021 (2013).
90. Deutsch, C. A. *et al.* Impacts of climate warming on terrestrial ectotherms across latitude. *Proc. Natl. Acad. Sci. USA* **105**, 6668–6672. https://doi.org/10.1073/pnas.0709472105 (2008).
91. Bonamour, S., Chevin, L. M., Charmantier, A. & Teplitsky, C. Phenotypic plasticity in response to climate change: the importance of cue variation. *Phil. Trans. R. Soc. B* **374**, 20180178. https://doi.org/10.1098/rstb.2018.0178 (2019).
92. Bitter, M. C., Kapsenberg, L., Silliman, K., Gattuso, J. P. & Pfister, C. A. Magnitude and predictability of pH fluctuations shape plastic responses to ocean acidification. *Am. Nat.* **197**, 486–501 (2021).
93. Rivadeneira, M. & Fernández, M. Shifts in southern endpoints of distribution in rocky intertidal species along the south-eastern Pacific coast. *J. Biogeogr.* **32**, 203–209. https://doi.org/10.1111/j.1365-2699.2004.01133.x (2005).
94. Bakun, A. *et al.* Anticipated effects of climate change on coastal upwelling ecosystems. *Curr. Clim. Change Rep.* **1**, 85–93. https://doi.org/10.1007/s40641-015-0008-4 (2015).
95 Turi, G., Gruber, N. & Munnich, M. Climatic modulation of recent trends in ocean acidification in the California Current System. *Environ. Res. Lett.* **11**, 0140072016. https://doi.org/10.1088/1748-9326/11/1/014007 (2016).
96. Xiu, P. *et al.* Future changes in coastal upwelling ecosystems with global warming: the case of the California Current System. *Sci. Rep.* **8**, 2866. https://doi.org/10.1038/s41598-018-21247-7 (2018).
97. Agostini, S. *et al.* Simplification, not "tropicalization", of temperate marine ecosystems under ocean warming and acidification. *Glob. Change Biol.* **27**, 4771–4784. https://doi.org/10.1111/gcb.15749 (2021).
98. Garreaud, R. D. *et al.* VOCALS-CUpEx: the Chilean upwelling experiment. *Atmos. Chem. Phys.* **11**, 2015–2029. https://doi.org/10.5194/acp-11-2015-2011 (2011).
99. Pulgar, J. M. *et al.* Impact of oceanic upwelling on morphometric and molecular indices of an intertidal fish *Scartichthys viridis* (Blenniidae). *Mar. Freshw. Behav. Physiol.* **44**, 33–42. https://doi.org/10.1080/10236244.2010.533512 (2011).
100. Pérez-Matus, A. *et al.* Exploring the effects of fishing pressure and upwelling intensity over subtidal kelp forest communities in Central Chile. *Ecosphere* **8**, e01808. https://doi.org/10.1002/ecs2.1808 (2017).
101. Meneghesso, C. *et al.* Remotely-sensed L4 SST underestimates the thermal fingerprint of coastal upwelling. *Rem. Sen. Environ.* **237**, 111588. https://doi.org/10.1016/j.rse.2019.111588 (2020).
102. Box, G. E. P., Jenkins, G. M. & Reinsel, G. C. *Time Series Analysis: Forecasting and Control* 3rd edn. (Prentice-Hall, 1994).
103. Broitman, B. R., Blanchette, C. A. & Gaines, S. D. Recruitment of intertidal invertebrates and oceanographic variability at Santa Cruz Island. *California. Limnol. Oceanogr.* **50**, 1473–1479. https://doi.org/10.4319/lo.2005.50.5.1473 (2005).
104. Haraldsson, C. *et al.* Rapid, high-precision potentiometric titration of alkalinity in ocean and sediment pore waters. *Deep-Sea Res. Part.* **I**(44), 2031–2044. https://doi.org/10.1016/S0967-0637(97)00088-5 (1997).
105. Pierrot, D., Lewis, E. & Wallace, D. W. R. *MS Excel Program Developed for CO_2 System Calculations., ORNL/CDIAC-105.* Carbon Dioxide Information Analysis Center Oak Ridge, National Laboratory US Department of Energy. Oak Ridge Tennessee (2006).
106. Angilletta, M. J. Estimating and comparing thermal performance curves. *J. Thermal Biol.* **31**, 541–545. https://doi.org/10.1016/j.jtherbio.2006.06.002 (2006).

107. Gilchrist, G. W. A quantitative genetic analysis of thermal sensitivity in the locomotor performance curve of *Aphidus ervi*. *Evolution* **50**, 1560–1572. https://doi.org/10.1111/j.1558-5646.1996.tb03928.x (1996).

Acknowledgements
We would like to thank Luis Prado for field and laboratory assistance. This work was funded by FONDECYT Grant No. 1240367 and N°1221322 to MAL and NAL and N°1221699 to BRB. Also, this work was partially funded by ANID–Millennium Science Initiative Program–Code ICN2019_015 and ANILLO 240004. We would also like to thank the reviewers for their constructive comments, which helped improve the article.

Author contributions
Marco A. Lardies: Writing – original draft, editing, Methodology, Formal analysis, Conceptualization Supervision, Resources. María Poupin: Writing – original draft, Methodology, Investigation, Formal analysis, Data curation. Nelson Lagos: Investigation, Methodology, Data curation, Funding acquisition, writing – review & editing. Bernardo Broitman: Methodology, Investigation, Formal analysis, Funding acquisition, writing – review & editing. Carolina Fernández: Methodology, Investigation, writing – review & editing, Conceptualization.

Competing interests
The authors declare no competing interests.

Ethical approval
All procedures were conducted in accordance with the Research Ethics guidelines of ANID-Chile (2019) and were approved by the Bioethics Committee of Adolfo Ibáñez University (No. 20/2019). Additionally, all protocols used in this study adhere to the ARRIVE guidelines for hydrobiological species.

Additional information
Correspondence and requests for materials should be addressed to M.A.L.

Reprints and permissions information is available at www.nature.com/reprints.

Publisher's note Springer Nature remains neutral with regard to jurisdictional claims in published maps and institutional affiliations.